

Dynam ic nuclear polarization induced by breakdown of fractional quantum Hall effect

M. Kawamura,^{1,2} M. Ono,¹ Y. Hashimoto,³ S. Katsumoto,^{3,4} K. Hamaya,^{1,4} and T. Machida^{1,4,y}¹Institute of Industrial Science, University of Tokyo,
4-6-1 Komaba, Meguro-ku, Tokyo 153-8505, Japan²PRESTO, Japan Science and Technology Agency, 4-1-8 Kawaguchi, Saitama 333-0012, Japan³Institute for Solid State Physics, University of Tokyo,
5-1-5 Kashiwanoha, Kashiwa 277-8581, Japan⁴Institute for Nano Quantum Information Electronics,
University of Tokyo, 4-6-1 Komaba, Meguro-ku, Tokyo 153-8505, Japan

(Dated: February 12, 2022)

We study dynam ic nuclear polarization (DNP) induced by breakdown of the fractional quantum Hall (FQH) effect. We find that voltage-current characteristics depend on current sweep rates at the quantum Hall states of Landau level filling factors $\nu = 1, 2/3$, and $1/3$. The sweep rate dependence is attributed to DNP occurring in the breakdown regime of FQH states. Results of a pump and probe experiment show that the polarities of the DNP induced in the breakdown regimes of the FQH states is opposite to that of the DNP induced in the breakdown regimes of odd-integer quantum Hall states.

Two-dimensional electron systems (2DESs) subjected to perpendicular magnetic fields exhibit the integer quantum Hall effect (QHE) with vanishing longitudinal resistance and quantized Hall resistance¹. When a bias current applied to a 2DES exceeds a critical current (I_c), the quantum Hall conductor becomes unstable against the excitation of electron-hole pairs, and therefore, the longitudinal resistance increases abruptly^{2,3,4,5}. This phenomenon is referred to as the QHE breakdown.

In the case of breakdown of a quantum Hall (QH) state with an odd-integer Landau level filling factor, electrons in the spin-up Landau subband are excited to the spin-down subband, along with up-to-down flips of electron spins. Since electron spins S interact with nuclear spins I via the hyperfine interaction $H_{\text{hyperfine}} = AS \cdot I = A(S^+ I^- + S^- I^+) = 2AS_z I_z$, where A is the hyperfine constant, electron spin flips cause nuclear spin flips. Dynam ic nuclear polarization (DNP) in the breakdown of odd-integer QH states has been demonstrated in our recent studies^{6,7}. Nuclear spins are polarized in the bulk part of the 2DES, as shown by an experiment using a device with Corbino geometry⁸.

Recent studies have revealed that fractional quantum Hall (FQH) states also break down when a bias current exceeds I_c ^{9,10}. Since the origin of the FQH effect, which is Coulomb interaction, is different from that of the integer QHE, it is unclear whether DNP also occurs in the breakdown regimes of FQH states. Furthermore, in FQH states, competition between the exchange energy and the Zeeman energy leads to the production of a wide variety of ground states with different electron spin configurations¹. The different configurations are expected to give rise to different DNP polarities.

In this paper, we report that DNP occurs in the breakdown regimes of FQH states at $\nu = 2/3$ and $1/3$. Results of our study indicate that voltage-current characteristics depend on current sweep rates. The relationship between DNP and the sweep rate dependence is confirmed by nuclear magnetic resonance (NMR) measurements. Fur-

thermore, we determine the polarity and amplitude of the DNP by a pump and probe experiment. The DNP polarity is unexpectedly negative ($\hbar I_z < 0$) and is opposite to the polarity of DNP induced in the breakdown regimes of odd-integer QH states⁶.

We used a GaAs/Al_{0.3}Ga_{0.7}As single heterostructure wafer with a 2DES at the interface. The mobility and sheet carrier density of the 2DES at 4.2 K were $\mu = 228 \text{ m}^2 \text{ V}^{-1} \text{ s}^{-1}$ and $n = 1.59 \times 10^{15} \text{ m}^{-2}$, respectively. The wafer was processed into a 20- μm -wide Hall bar covered with a front-gate electrode, as shown in Fig. 1 (a). This electrode was used to change the Landau level filling factor of the 2DES. Figure 1 (b) shows a gray-scale plot of the longitudinal resistance R_{xx} as a function of the external magnetic field B and Landau level filling factor ν . The resistance peaks observed in the $\nu = 2/3$ FQH state

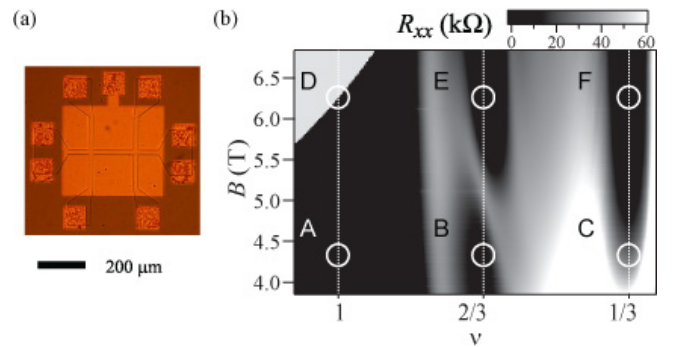


FIG. 1: (Color online) (a) Micrograph of the Hall bar device used in the present study. (b) Gray-scale plot of the longitudinal resistance R_{xx} as a function of the external magnetic field B and the Landau level filling factor ν at 20 mK. R_{xx} was measured by using a standard ac lock-in technique at an excitation current of $I_{ac} = 1 \text{ nA}$ (18 Hz). The black regions represent quantum Hall states. Pump and probe measurements were performed at the conditions indicated by circles (A to F).

at around $B = 5.2$ T correspond to the spin transition, as reported in previous studies^{12,13}. The QH states on the low and high magnetic field sides of the transition are spin-unpolarized and spin-polarized phases, respectively.

The dashed curve in the inset of Fig. 2 (a) represents a voltage-current (V_{xx} - I) characteristic curve at $B = 6.26$ T and $\nu = 1$ [cf. in Fig. 1 (b)]. The current was increased at a rate of 6.8 nA/s. When the bias current I exceeds a critical value $I_c = 1.4$ A, the longitudinal voltage V_{xx} increases abruptly. As mentioned earlier, this phenomenon is referred to as the QHE breakdown. The V_{xx} - I characteristic curve represented by the solid curve in the inset of Fig. 2 (a) was obtained by increasing the current with a sweep rate of 0.4 nA/s. The QHE breaks down at a smaller I_c when the sweep rate is decreased. The sweep rate dependence of the V_{xx} - I characteristic can be attributed to the DNP, as in the case of the hysteretic V_{xx} - I curves in our previous study⁶: In the breakdown regimes of odd-integer QH states, electrons are excited to higher Landau levels, and nuclear spins are dynamically polarized by the up-to-down flips of electron spins. The polarized nuclear spins reduce the spin-splitting energy $E_s = \hbar \gamma \mu_B B$, where γ is the effective g -factor of electrons ($\gamma = 0.44$ in GaAs) and μ_B is the Bohr magneton. Since the energy gap of odd-integer QH states is given by the sum of E_s and exchange energy, the reduction of E_s accelerates the QHE breakdown, resulting in the shift of V_{xx} - I curves toward the low current side⁶.

Figure 2 (a) shows the V_{xx} - I curves obtained in the case of a spin-polarized FQH state at $B = 6.26$ T and $\nu = 2/3$ [cf. in Fig. 1 (b)]. The current sweep rates were 6.8 nA/s and 0.05 nA/s for the dashed and solid curves, respectively. As observed at $\nu = 1$, V_{xx} increases when the current exceeds a critical value. This indicates the breakdown of the FQH effect. The FQH effect breaks down at a larger I_c when the sweep rate is decreased. The sweep-rate-dependent V_{xx} - I characteristics appear similar to those observed in the breakdown regime of the $\nu = 1$ QH state, except for the direction of the shift of the V_{xx} - I curves. Figure 2 (b) shows the time evolution of V_{xx} at the $\nu = 2/3$ spin-polarized FQH state after a sudden increase in I from 0 nA to 30 nA. The value of V_{xx} decreases slowly over a period of 600 s, which is a typical time scale for nuclear spin related phenomena^{6,14,15,16}. Thus, the slow evolution of V_{xx} and the sweep-rate-dependent V_{xx} - I curves indicate that DNP occurs in the breakdown regime of the FQH state.

The relationship between the DNP and the sweep-rate-dependent V_{xx} - I characteristics and slow evolution of V_{xx} was determined by NMR measurements as follows. In order to apply a radio-frequency (rf) magnetic field B_{rf} perpendicular to the external magnetic field B (parallel to the 2DES), we wound a single-turn coil around the Hall bar device. As the frequency of B_{rf} was scanned, V_{xx} peaked at the NMR frequencies of ^{75}As , as shown in Fig. 2 (c). NMR spectra of ^{69}Ga and ^{71}Ga were also obtained. Similar sweep-rate dependence in V_{xx} - I characteristics and NMR were observed at all the QH states

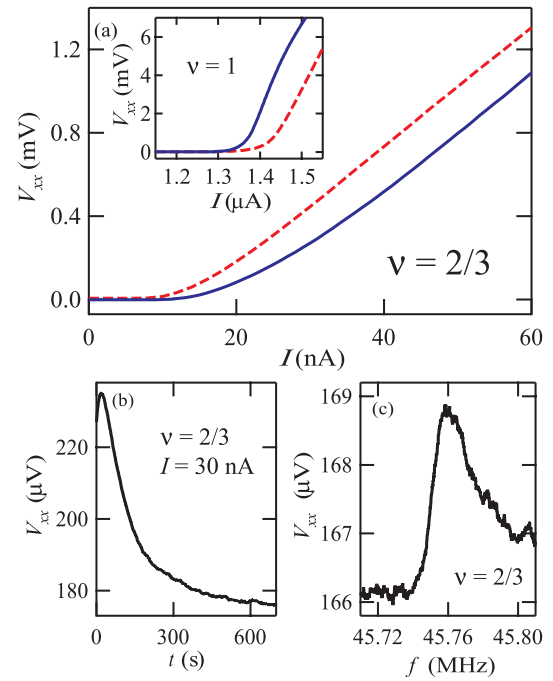


FIG. 2: (Color online) (a) V_{xx} - I curves obtained at $\nu = 2/3$ and $B = 6.26$ T [cf. in Fig. 1 (b)]. The current sweep rates were 6.8 nA/s (dashed) and 0.05 nA/s (solid). The inset shows V_{xx} - I curves obtained at $\nu = 1$ and $B = 6.26$ T [cf. in Fig. 1 (b)] with current sweep rates of 6.8 nA/s (dashed) and 0.4 nA/s (solid). (b) Time evolution of V_{xx} after a sudden increase in I from 0 nA to 30 nA. (c) NMR spectrum of ^{75}As detected by measuring V_{xx} at $\nu = 2/3$ and $I = 30$ nA.

investigated [A to F in Fig. 1 (b)]. The detection of NMR by the voltage measurements definitely revealed the occurrence of DNP in the breakdown regimes of the FQH states.

It should be noted that the DNP observed in this study is different from the well-known DNP^{16,17,18,19,20,21} occurring near the spin transition at $\nu = 2/3$. It has been suggested that the DNP near the spin transition is induced by electron scattering between spatially distributed spin-polarized and spin-unpolarized domains^{17,18}. Therefore, the coexistence of spin-polarized and spin-unpolarized domains is considered a prerequisite for the DNP near the spin transition. In contrast, the DNP observed in this study occurs in the breakdown regime of the FQH states away from the spin transition point. In the condition, spin configuration of the FQH system is not affected by the spin transition and the complex spin-domain structure does not exist. We think that a mechanism other than the inter-spin-domain scattering^{17,18} is needed to understand the DNP observed in this study.

As shown in Fig. 2 (a), the V_{xx} - I curves shift as the DNP occurs. The directions of the shifts at $\nu = 2/3$ and $\nu = 1$ are opposite to each other; this indicates that the DNP polarities are different. Therefore, in order to investigate the polarities of DNP more systematically, we con-

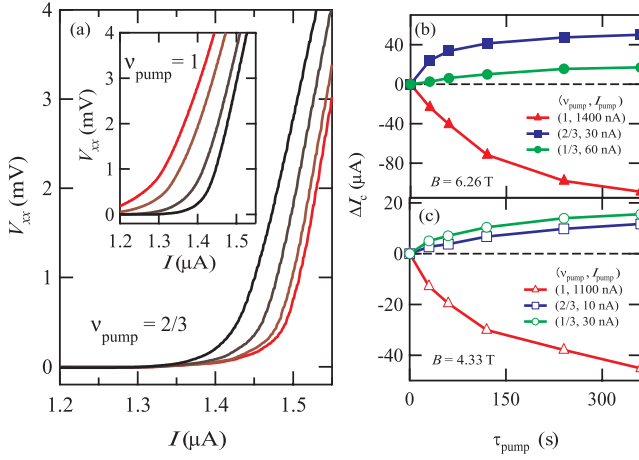


FIG. 3: (Color online) (a) V_{xx} - I curves obtained at $\nu = 1$ and $B = 6.26$ T after inducing DNP at $(\nu_{\text{pump}}, I_{\text{pump}}) = (2/3, 30$ nA) for τ_{pump} values of 0, 30, 120, and 360 s (from left to right). Inset: V_{xx} - I curves obtained at $\nu = 1$ after inducing DNP at $(\nu_{\text{pump}}, I_{\text{pump}}) = (1, 1400$ nA). The values of τ_{pump} are 0, 30, 120, and 360 s from right to left. (b) Horizontal shift I_c of V_{xx} - I curves defined at $V_{xx} = 2$ mV plotted as a function of τ_{pump} at $B = 6.26$ T. Results obtained at $(\nu_{\text{pump}}, I_{\text{pump}}) = (1, 1400$ nA), $(2/3, 30$ nA), and $(1/3, 60$ nA) are represented by solid triangles, solid squares, and solid circles, respectively. (c) Similar data obtained at $B = 4.33$ T. Results obtained at $(\nu_{\text{pump}}, I_{\text{pump}}) = (1, 1100$ nA), $(2/3, 10$ nA), and $(1/3, 30$ nA) are represented by open triangles, open squares, and open circles, respectively.

ducted the pump and probe experiment: First, the 2DES was temporarily set to a breakdown state $(\nu_{\text{pump}}; I_{\text{pump}})$ for a duration τ_{pump} in order to induce DNP. Next, the bias current was turned on, and the filling factor was suddenly changed to $\nu_{\text{probe}} = 1$ by using the front-gate electrode. Then, the I_c value of the $\nu_{\text{probe}} = 1$ QH state was measured by increasing the bias current²². Since the I_c value is expected to change in accordance with $hI_z i$, we can determine the polarity and amplitude of DNP induced at ν_{pump} ²³.

The inset of Fig. 3 (a) shows V_{xx} - I curves obtained at $\nu = 1$ after inducing DNP at $(\nu_{\text{pump}}, I_{\text{pump}}) = (1, 1400$ nA) and $B = 6.26$ T [D in Fig. 1 (b)] for several values of τ_{pump} . The rightmost curve (black) represents the results obtained without inducing DNP ($\tau_{\text{pump}} = 0$ s), and the leftmost curve (red) represents the results obtained after inducing DNP for $\tau_{\text{pump}} = 360$ s. The horizontal shift I_c of the V_{xx} - I curve defined at $V_{xx} = 2$ mV is plotted as a function of τ_{pump} [closed triangles in Fig. 3 (b)]. I_c decreases with increasing τ_{pump} . This indicates that the decrease in I_c can be attributed to the DNP.

The main panel of Fig. 3 (a) shows V_{xx} - I curves obtained at $\nu = 1$ after inducing DNP at $(\nu_{\text{pump}}, I_{\text{pump}}) = (2/3, 30$ nA) and $B = 6.26$ T [E in Fig. 1 (b)] for several values of τ_{pump} . The curves shift to higher currents with increasing τ_{pump} . The τ_{pump} dependence of I_c is indicated by solid squares in Fig. 3 (b). I_c increases with

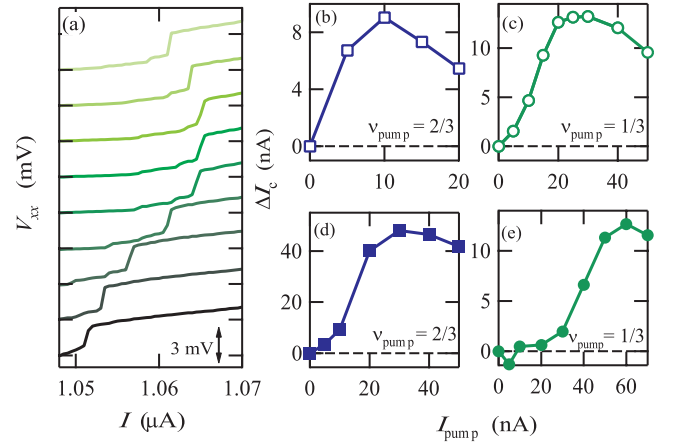


FIG. 4: (a) V_{xx} - I curves obtained after inducing DNP at $(\nu_{\text{pump}}, B) = (1/3, 4.33$ T) and $\nu_{\text{pump}} = 600$ s with different pump currents: $I_{\text{pump}} = 0, 5, 10, 15, 20, 25, 30, 40,$ and 50 nA (from bottom to top). The curves are offset vertically for clarity. (b)-(e) Horizontal shift I_c of V_{xx} - I curves plotted as a function of I_{pump} at $(\nu_{\text{pump}}, B) = (2/3, 4.33$ T), $(1/3, 4.33$ T), $(2/3, 6.26$ T), and $(1/3, 6.26$ T), respectively.

τ_{pump} . It should be noted that I_c decreases when an rf magnetic field with NMR frequency is applied. Therefore, the nonzero values of I_c indicate that DNP occurs in the breakdown regimes of the FQH states²⁴. Data obtained on the spin-unpolarized phase at $B = 4.33$ T [B in Fig. 1 (b)] are shown by open squares in Fig. 3 (c). The sign of I_c is also positive for $B = 4.33$ T. Similar data obtained for $\nu_{\text{pump}} = 1/3$ at $B = 6.26$ T [F in Fig. 1 (b)] are shown by solid circles in Fig. 3 (b). In this case also, I_c increases with τ_{pump} .

Figure 4 (a) shows V_{xx} - I curves obtained after inducing DNP at $(\nu_{\text{pump}}, B) = (1/3, 4.33$ T) and several values of I_{pump} for $\nu_{\text{pump}} = 600$ s. The V_{xx} - I curves shift horizontally with increasing I_{pump} . The values of I_c are plotted as a function of I_{pump} in Fig. 4 (c) (open circles). The horizontal shift I_c is maximum at $I_{\text{pump}} = 30$ nA. Qualitatively similar data are obtained for $(\nu_{\text{pump}}, B) = (2/3, 4.33$ T), $(2/3, 6.26$ T), and $(1/3, 6.26$ T), as shown in Figs. 4 (b), (d), and (e), respectively. In all cases, the amplitude of DNP increases steeply when I_{pump} exceeds I_c and is maximum when I_{pump} is slightly greater than I_c . The I_{pump} dependence of DNP in the breakdown regime of FQH states is similar to that observed in the breakdown regime of odd-integer QH states⁸. This similarity indicates that the origin of DNP occurring in the breakdown regimes of both FQH and odd-integer QH states is the same.

We discuss the polarities of the DNPs occurring in the breakdown regimes of the FQH states. The positive signs of the I_c values for $\nu_{\text{pump}} = 2/3$ and $1/3$ are opposite to those for $\nu_{\text{pump}} = 1$. The positive sign of I_c value shows that the energy gap of the $\nu_{\text{probe}} = 1$ QH state increases due to DNP. Since $E_s = \nu j_B B = \nu hI_z i$ increases due to negative DNP ($hI_z i < 0$), DNP with negative polarity

is deduced from the positive I_c value. The results in Figs. 3(b) and 3(c) show that DNPs with negative polarities are induced in the breakdown regimes of $\nu_{\text{pump}} = 1/3$ and $\nu_{\text{pump}} = 2/3$.

The negative DNPs for $\nu_{\text{pump}} = 1/3$, opposite to the DNPs for $\nu_{\text{pump}} = 1$, are unexpected because electron spins are fully polarized in both ground states. Furthermore, for $\nu_{\text{pump}} = 2/3$, the signs of DNPs are the same (negative) both on the spin-unpolarized phase at 4.33 T and on the spin-unpolarized phase at 6.26 T [B and E in Fig. 1(b), respectively], despite of the difference in electron spin configurations in the ground states. These results suggest that neither electron spin configurations

in the FQH ground states nor spin transitions are relevant to the polarity of DNP occurring in the breakdown regimes. In the breakdown regime, a number of electron-hole pairs are excited in the 2DES and the electron spin configurations of the FQH ground states, which is based on subtle electron-electron correlation, are probably not maintained. We infer that spin dynamics of these excitations plays an important role to understand the mechanism of the DNPs occurring in the breakdown regimes.

This study is supported by a Grant-in-Aid from MEXT, the Sumitomo Foundation, and the Special Coordination Funds for Promoting Science and Technology.

Present address: Advanced Science Institute, RIKEN, 2-1 Wako, Saitama 351-0198, Japan; Electronic address: monu@riken.jp

^y Electronic address: tmachida@iis.u-tokyo.ac.jp

- ¹ For a review, see T. Chakraborty and P. Pietiläinen, *The Quantum Hall Effects: Integral and Fractional*, 2nd ed. (Springer-Verlag, Berlin, 1995).
- ² G. Ebert, K. von Klitzing, K. P. Bog, and G. Weimann, *J. Phys. C* **16**, 5441 (1983).
- ³ M. E. Cage, R. F. Dziuba, B. F. Field, E. R. Williams, S. M. Girvin, A. C. Gossard, D. C. Tsui, and R. J. Wagner, *Phys. Rev. Lett.* **51**, 1374 (1983).
- ⁴ G. N. Aichtweil, *Physica E* **4**, 79 (1999).
- ⁵ S. Komiyama and Y. Kawaguchi, *Phys. Rev. B* **61**, 2014 (2000).
- ⁶ M. Kawamura, H. Takahashi, K. Sugihara, S. Masubuchi, K. Hayama, and T. Machida, *Appl. Phys. Lett.* **90**, 022102 (2007).
- ⁷ H. Takahashi, M. Kawamura, S. Masubuchi, K. Hamaya, T. Machida, Y. Hashimoto, and S. Katsumoto, *Appl. Phys. Lett.* **91**, 092120 (2007).
- ⁸ M. Kawamura, H. Takahashi, S. Masubuchi, Y. Hashimoto, S. Katsumoto, and T. Machida, *J. Phys. Soc. Jpn.* **77**, 023710 (2008).
- ⁹ T. Takamasu, H. Dodo, and N. Miura, *Solid State Commun.* **96**, 121 (1995).
- ¹⁰ J. P. Watts, A. Usher, A. J. Matthews, M. Zhu, M. Elliott, W. G. Herrenden-Harker, P. R. Morris, M. Y. Simmons, and D. A. Ritchie, *Phys. Rev. Lett.* **81**, 4220 (1998).
- ¹¹ S. M. Girvin and A. H. MacDonald, in *Perspectives on Quantum Hall Effect*, edited by S. Das Sarma and A. Pinczuk, 161{224 (Wiley, New York, 1996).

- ¹² J. P. Eisenstein, H. L. Stormer, L. Pfeiffer, and K. W. West, *Phys. Rev. Lett.* **62**, 1540 (1989).
- ¹³ L. W. Engel, S. W. Hwang, T. Sajto, D. C. Tsui, and M. Shayegan, *Phys. Rev. B* **45**, 3418 (1992).
- ¹⁴ A. M. Song and P. Omling, *Phys. Rev. Lett.* **84**, 3145 (2000).
- ¹⁵ T. Machida, T. Yamazaki, and S. Komiyama, *Appl. Phys. Lett.* **82**, 409 (2003).
- ¹⁶ S. Kronmüller, W. Dietsche, J. Weis, K. von Klitzing, W. Wegscheider, and M. Bichler, *Phys. Rev. Lett.* **81**, 2526 (1998).
- ¹⁷ S. Kronmüller, W. Dietsche, K. von Klitzing, G. Denninger, W. Wegscheider, and M. Bichler, *Phys. Rev. Lett.* **82**, 4070 (1999).
- ¹⁸ S. Kraus, O. Stern, J. G. S. Lok, W. Dietsche, K. von Klitzing, M. Bichler, D. Schuh, and W. Wegscheider, *Phys. Rev. Lett.* **89**, 266801 (2002).
- ¹⁹ O. Stern, N. Freytag, A. Fay, W. Dietsche, J. H. Smet, K. von Klitzing, D. Schuh, and W. Wegscheider, *Phys. Rev. B* **70**, 075318 (2004).
- ²⁰ K. Hashimoto, K. Muraki, T. Saku, and Y. Hirayama, *Phys. Rev. Lett.* **88**, 176601 (2002).
- ²¹ K. Hashimoto, T. Saku, and Y. Hirayama, *Phys. Rev. B* **69**, 153306 (2004).
- ²² The current was increased rapidly so that DNP during the current sweep was negligible.
- ²³ DNPs induced at various ν_{pump} were detected at the fixed $\nu_{\text{probe}} = 1$ so that we can discuss the relative polarities and amplitudes of the DNPs.
- ²⁴ Electron heating effect leads to a decrease in the critical current I_c , whereas I_c increases in the present experiment.